

The Effects of Grooves on the Flow Rate in a Microchannel

Hyun-Jin Hwang¹ & Simon Song¹

¹Department of Mechanical Engineering, Hanyang University, Seoul 133-791, Korea

Correspondence and requests for materials should be addressed to S. Song (simonsong@hanyang.ac.kr)

Accepted 15 April 2008

Abstract

The pressure drop along a microchannel is significantly larger than in a macrochannel because of increased frictional drag. In order to reduce the frictional drag, various geometries have been studied by patterning microribs or protrusions on a microchannel bottom. However, using numerical simulations, we investigate the effects of grooves located on the side wall of a channel on the flow rate. Numerical results show that the flow rate is influenced considerably by the number, size, and shape of the grooves.

Keywords: Drag reduction, Microchannel, Groove, Flow rate

Introduction

Microfluidics concerns fluid behavior and flow control in a microchannel, and is a core technology for the commercialization of a micro Total analysis system (μ -TAS) or Lab-on-a-chip (LOC)¹⁻⁴. As the demand for microfluidic chips increases, an understanding of the flow characteristics in a microchannel is required. However, a fluid flow at the micro- or nanoscales exhibits characteristics different from those of a macroscale flow⁵⁻⁷. For example, a fluid flow driven by a pressure gradient exhibits an increased pressure drop along a channel for a given flow rate because the pressure drop is inversely proportional to the forth power of the channel dimension^{7,8}. In addition, the ratio of surface area to volume increases significantly as the scale of the device decreases. Thus, flow resistance increases due to friction between the channel surface and fluid, affecting the flow rate¹⁻⁹.

To reduce the flow resistance in a microchannel, two types of approaches have been studied. One approach is to change the surface characteristics into a slip condition using a chemical treatment¹⁰. However,

this method is difficult to apply to a rough surface¹. The other approach is to fabricate a superhydrophobic surface in the microchannel^{5-7,11-17}. This approach is based on the idea of the lotus leaf effect in which a water droplet on a leaf forms a bead and slips off without wetting. The lotus leaf surface is composed of nanoscale protrusions on microscale bumps. Since the contact area of the droplet on the lotus leaf is quite small due to this surface structure and the layer of air caught between protrusions, the droplet tumbles down without friction. To realize the idea, many researchers have patterned cavities or microribs in a microchannel. Davies *et al.*⁷ and Choi *et al.*^{11,15} fabricated a microchannel of which the upper and bottom surfaces have microribs or cavities arranged transverse to the flow direction. Ou *et al.*^{5,14} reported on a microchannel with cubic microposts on the bottom or shear-free bands parallel to the flow direction, and controlled the contact area between the fluid and

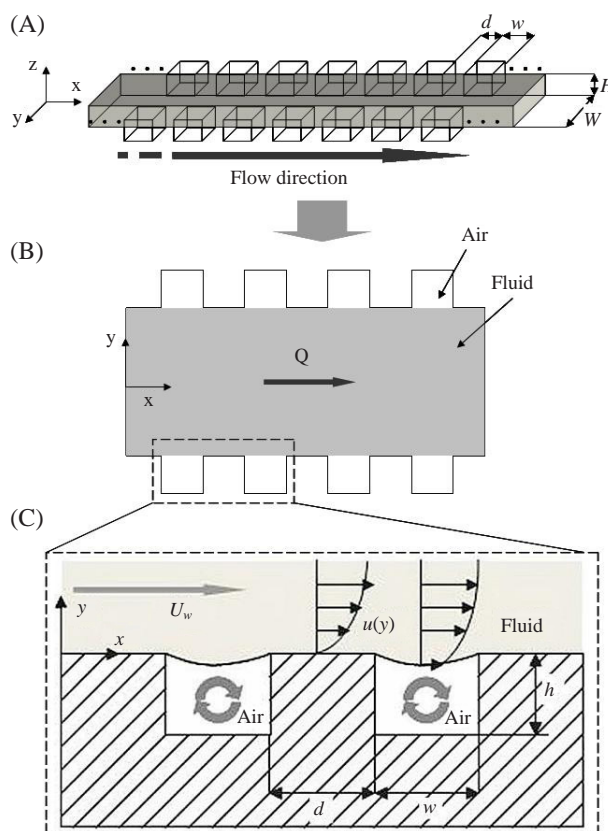


Figure 1. Schematic diagrams of (A) a microchannel, (B) the top view of microchannel, and (C) boundary conditions.

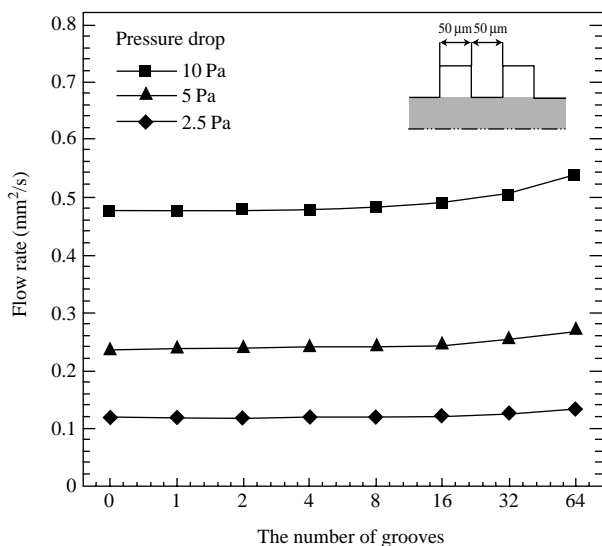


Figure 2. Flow rate variation with respect to the number of grooves for various pressure drops.

channel surfaces. They insisted that they reduced the flow resistance by 40%. However, these methods would be ineffective if the ratio of channel height to width is greater than one.

We investigate the effects of grooves located on the side walls of a microchannel on the flow rate for a given pressure drop by using numerical simulations. The flow geometry is shown in Figure 1. The microchannel is assumed to be 7 mm long, 200 μm wide, and 150 μm high. The groove spacing (d) is 50 μm , and the width (w) is 50 μm . The grooves contain air, and the microchannel is filled with water. A no-slip condition is applied to the channel walls while a slip condition is used at the interface between the air and water.

Results and Discussion

Effects of the Number of Grooves

Using numerical simulations, we examined the flow fields for different numbers of grooves. The numbers of grooves were varied by the second power of 2. The groove length and width were 50 μm . The pressure drops applied along the microchannel were 2.5, 5, and 10 Pa. Figure 2 shows the flow rate with respect to the number of grooves in the microchannel. The flow rate increases by about 13% in a microchannel with 64 grooves and a pressure drop of 10 Pa, as compared to a channel without grooves. Also, the results indicate that the number of grooves affects the flow rate more significantly as the pressure drop increases.

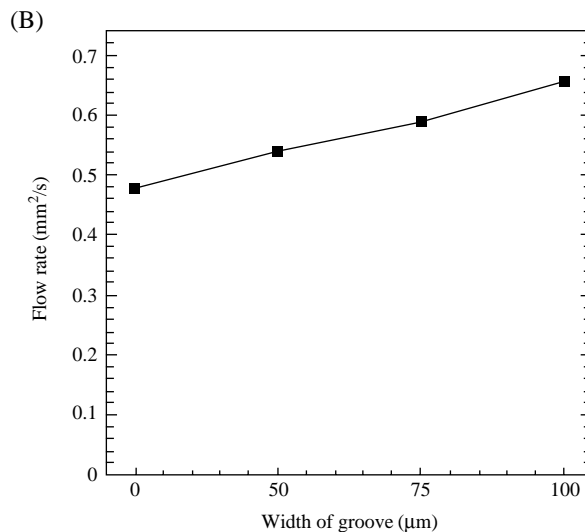
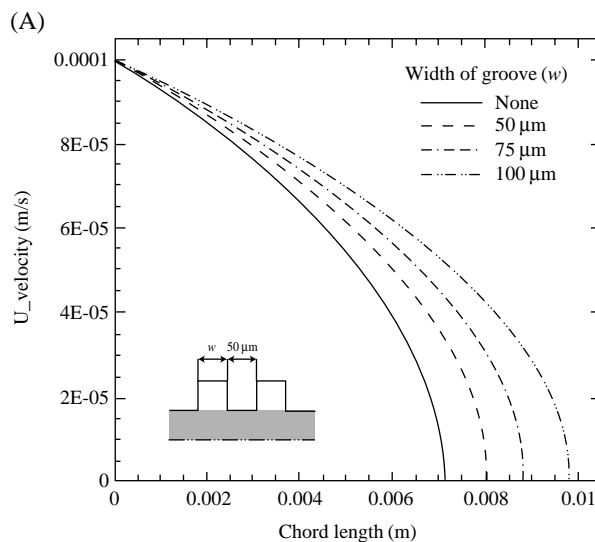


Figure 3. (A) Velocity profile and (B) flow rate with respect to groove width: The pressure drop is fixed at 10 Pa.

Effects of the Groove Width

In order to investigate the effects of groove size on the flow rate, the groove width was changed to 50, 75, and 100 μm . The pressure drop was fixed at 10 Pa along the channel. Figure 3(A) shows the velocity profiles near the outlet. As the groove width increases, the maximum velocity also increases. The flow rate increases linearly with increasing the groove width, as shown in Figure 3(B). Compared to a channel without grooves, the flow rate increases by 37% for a groove width of 100 μm .

Effects of the Groove Shape

The effect of the groove shape was investigated

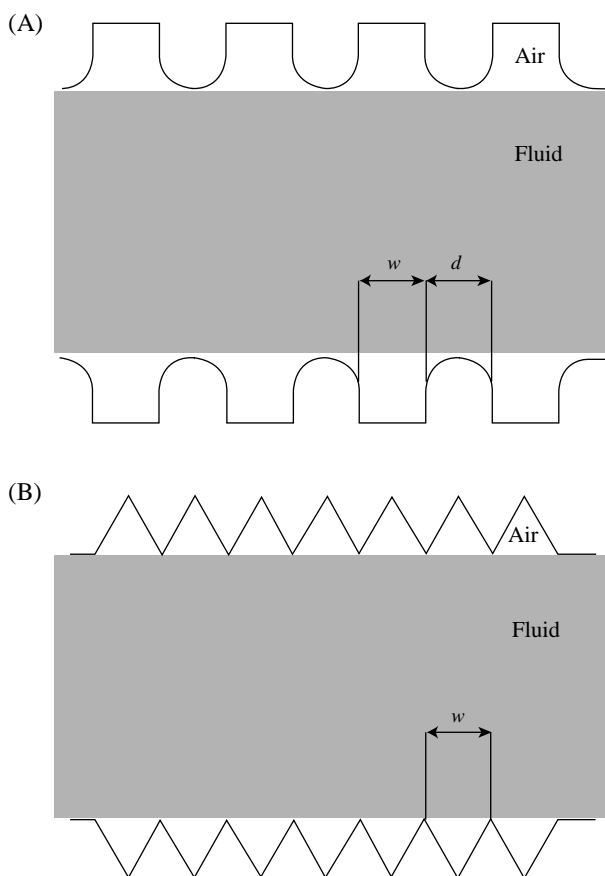


Figure 4. Schematics of microchannel with (A) semicircular groove ($w=50\ \mu\text{m}$ and $d=50\ \mu\text{m}$) and (B) triangular grooves ($w=50\ \mu\text{m}$).

using square, semicircular, and triangular grooves in the microchannels, as shown in Figure 4. The number of grooves in a channel with square and semicircular grooves was 64, while in a channel with triangular grooves the number was 127. The pressure drop between the inlet and outlet was fixed at 10 Pa. Figure 5(A) shows the velocity profiles near the outlet of a channel for the three groove shapes. The maximum velocity significantly increases in a channel with a smaller contact area between the fluid and channel walls. The flow rate for the triangular grooves is 180% and 149% greater than those for the smooth wall and square grooves, respectively. The flow rate for the semicircular grooves is 48% and 30% higher than those for the smooth wall and square grooves, respectively.

Conclusion

We examined the effects of grooves on the flow rate

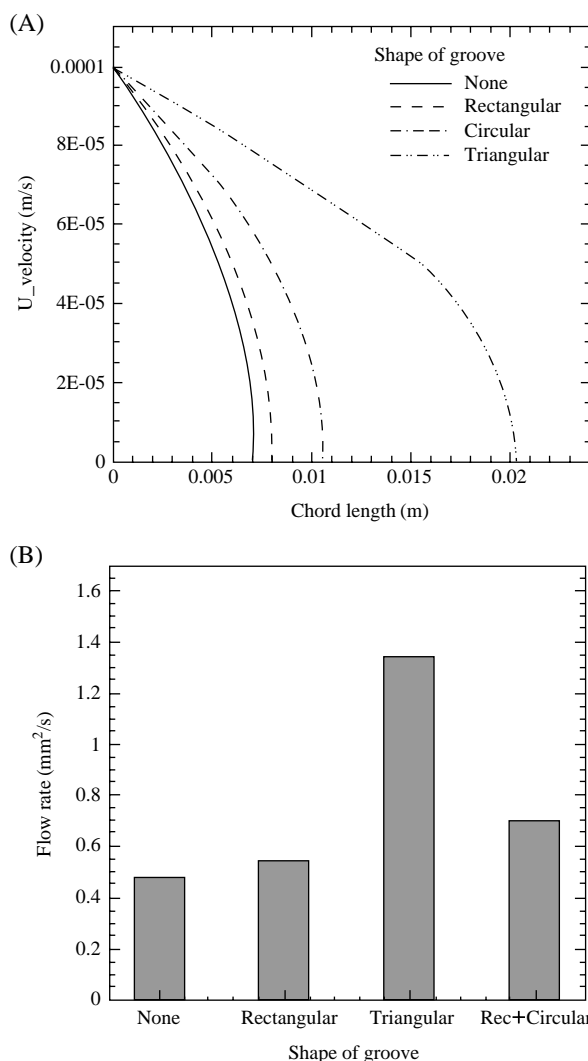


Figure 5. (A) Velocity profile and (B) flow rate with respect to groove shapes: The pressure drop is fixed at 10 Pa.

in a microchannel by changing the number, size, and shape of the grooves through numerical simulations. Unlike other studies, the grooves were located on the side-walls in this study. The results indicate that the flow rate increases with increasing the number of grooves and groove width. Also, the triangular grooves lead to a flow rate 180% greater than that for the case of a smooth wall. The results imply that grooves on the side-walls are effective in increasing the flow rate when the aspect ratio of channel height to width is greater than one.

Numerical Methods

In this study, a commercial CFD solver (CFD-ACE+; ESI US R & D Inc., Huntsville, AL, USA) was used. A 2-D model was adapted using a symmetric condi-

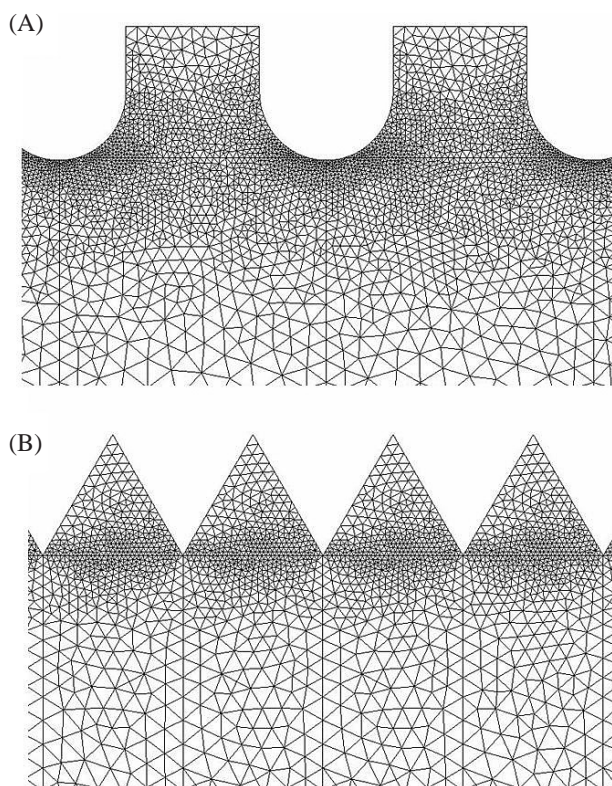


Figure 6. Generation of unstructured grid: (A) semicircular groove, and (B) triangular groove.

tion. Since the accuracy of a numerical analysis depends on the number of grids, a grid test was performed. As a result, the number of grids was fixed at around 200,000. A channel with square grooves was constructed using structured grids, while another channel with semicircular or triangular grooves was constructed using unstructured grids, as shown in Figure 6. The grid size near the interface between the fluid and air was adjusted to be relatively small in order to resolve a complicated flow. The flow properties are as follows: $\rho_{\text{water}}=1,000 \text{ kg/m}^3$, $\mu_{\text{water}}=0.001 \text{ kg/m} \cdot \text{s}$, $\rho_{\text{air}}=1.1614 \text{ kg/m}^3$, and $\mu_{\text{air}}=1.846\text{E}-05 \text{ kg/m} \cdot \text{s}$. A pressure boundary condition was applied at the inlet and outlet. In order to verify the numerical results, the flow in a smooth microchannel without grooves was simulated and compared to a theoretical Poiseuille flow. The results show good agreement between them.

Acknowledgements

This work was supported by the Korea Research Foundation Grant (KRF-2006-331-D00069) funded by the Korean Government (MOEHRD).

References

1. Kim, D.H. Microfluidic systems: State of the art. *Korean Chemical Engineering Research* **42**, 375-386 (2004).
2. Yea, C.H., Min, J.H. & Choi, J.W. The fabrication of cell chips for use as bio-sensors. *BioChip J.* **1**, 219-227 (2007).
3. Kim, P.N. *et al.* Soft lithography for microfluidics: a review. *BioChip J.* **2**, 1-11 (2008).
4. Hong, J.G. Microfluidic systems for high throughput screening. *BioChip J.* **2**, 12-26 (2008).
5. Ou, J.R. & Rothstein, J.P. Direct velocity measurements of the flow past drag-reducing ultrahydrophobic surfaces. *Physics of Fluids* **17**, 103606 (2005).
6. Cao, B.Y., Chen, M. & Guo, Z.Y. Liquid flow in surface-nanostructured channels studied by molecular dynamics simulation. *Phys. Rev. E* **74**, 066311 (2006).
7. Davies, J., Maynes, D., Webb, B.W. & Woolford, B. Laminar flow in a microchannel with superhydrophobic walls exhibiting transverse ribs. *Phys. of Fluids* **18**, 087110 (2006).
8. Judy, J., Maynes, D. & Webb, B.W. Characterization of frictional pressure drop for liquid flows through microchannels. *Int. J. Heat Mass Transf.* **45**, 3477-3489 (2002).
9. Ho, C.M. & Tai, Y.C. Micro-electro-mechanical-systems (MEMS) and fluid flows. *Annu. Rev. Fluid Mech.* **30**, 579-612 (1998).
10. Choi, C.H., Westin, K.J.A. & Breuer, K.S. Apparent slip flows in hydrophilic and hydrophobic microchannels. *Phys. of Fluids* **15**, 2897-2902 (2003).
11. Choi, C.H. & Kim, C.J. Large slip of aqueous liquid flow over a nanoengineered superhydrophobic surface. *Phys. Rev. Lett.* **96**, 066001 (2006).
12. Min, T.G. & Kim, J. Effects of hydrophobic surface on skin-friction drag. *Phys. of Fluids* **16**, L55-L58 (2004).
13. Sbragaglia, M. & Prosperetti, A. A note on the effective slip properties for microchannel flows with ultrahydrophobic surfaces. *Phys. of Fluids* **19**, 043603 (2007).
14. Ou, J., Perot, B. & Rothstein, J.P. Laminar drag reduction in microchannels using ultrahydrophobic surfaces. *Phys. of Fluids* **16**, 4635-4643 (2004).
15. Choi, C.H., Ulmanella, U., Kim, J., Ho, C.M. & Kim, C.J. Effective slip and friction reduction in nanogated superhydrophobic microchannels. *Phys. of Fluids* **18**, 087105 (2006).
16. Maynes, D., Jeffs, K., Woolford, B. & Webb, B.W. Laminar flow in a microchannel with hydrophobic surface patterned microribs oriented parallel to the flow direction. *Phys. of Fluids* **19**, 093603 (2007).
17. Cottin-Bizonne, C., Barrat, J.L., Bocquet, L. & Charlaix, E. Low-friction flows of liquid at nanopatterned interfaces. *Nat. Mater.* **2**, 237-240 (2003).